Potassium: A Tracer for Biomass Burning in Beijing?

Jinting Yu, Caiqing Yan, Yue Liu, Xiaoying Li, Tian Zhou, Mei Zheng[*]

SKL-ESPC and BIC-ESAT, College of Environmental Sciences and Engineering, Peking University, Beijing 100871, China

ABSTRACT

Potassium (K) is an important component of fine particulate matter (PM$_{2.5}$) and has been widely used as a tracer for biomass burning around the world. However, this may not be true in Beijing, where the sources of K are much more complicated. The aim of this research is to investigate whether K can be applied as a sole tracer for biomass burning in Beijing. From 2015 to 2016, the concentrations of K across the four seasons were measured by an Xact 625 monitor, which uses X-ray fluorescence, and the concentrations of K$^+$ during two seasons were measured by an in-situ Gas and Aerosol Composition (IGAC), which uses ion chromatography. It was found that the ratios of K/K$^+$ and K$^+$/PM$_{2.5}$ were close to that of coal combustion, and K exhibited good correlations with trace metals associated with coal combustion (e.g., Pb, As, Se, and Zn). The ratios of K/Pb during the peak of the haze episodes were very stable (around 15.70), suggesting the influence of a major but consistent source. Therefore, it was clear that coal combustion was one of the major sources of K in Beijing. To estimate the major source contributions to K, the ratios of K/Ca and K/Pb were used to represent dust and coal combustion, respectively. From this study, coal combustion was the major source of K (45–69%), followed by biomass burning and dust. However, a seasonality effect was observed, with the highest source contributions coming from coal combustion in winter (69%), biomass burning in autumn (49%), and dust in spring (19%). This research shows that biomass burning would be overestimated in Beijing using K as a sole tracer, since coal is also a major source of the latter.

Keywords: K; Tracer; Source; Biomass burning; Coal combustion.

INTRODUCTION

Potassium (K) is an important component of fine particulate matter (PM$_{2.5}$). There are multiple emission sources of K in the atmosphere, such as sea salt, cooking, dust, coal combustion, and waste incineration (Lawson *et al.*, 1979; Andreae, 1983; Waston *et al.*, 2001; Schauer *et al.*, 2002). Based on its water solubility, K can be classified into water-insoluble K and water-soluble K$^+$, which can be derived from different sources. Biomass burning is a primary source of K$^+$, mainly in the form of KCl, K$_2$SO$_4$ and KNO$_3$ (Li *et al.*, 2003). K emitted from sea salt also contributes to K$^+$ (Andreae, 1983; Duvall *et al.*, 2008). However, K emitted from soil and dust is mainly water-insoluble K, usually in the presence of aluminosilicate minerals (Andreae, 1983). Several studies have suggested that coal combustion could also emit K and K$^+$ into the atmosphere (Wang *et al.*, 2009, 2014).

K$^+$ has usually been used as the tracer for biomass

burning in receptor models (e.g., Chemical Mass Balance [CMB] Model, Positive Matrix Factorization [PMF], Principle Component Analysis [PCA], and so on) (Zhang *et al.*, 2013a, b; Tao *et al.*, 2014). However, in some studies, K was used as a substitute for tracing biomass burning sources, due to lack of K$^+$ measurement data (Song *et al.*, 2006; Yu *et al.*, 2013; Zheng *et al.*, 2014; Gao *et al.*, 2016; Zíková *et al.*, 2016). Several studies have also used ratios such as K$^+$/PM$_{2.5}$, EC/K$^+$ and K$^+$/OC to roughly estimate contributions of biomass burning to ambient aerosol (Duan *et al.*, 2004; Li *et al.*, 2007; Park *et al.*, 2013; Zhou *et al.*, 2017b). However, these methods were based on the assumption that K (or K$^+$) was solely derived from biomass burning and emission factors of K (or K$^+$) were not impacted by other conditions (e.g., fuel types and combustion conditions) (Yan *et al.*, 2017).

Although most studies have estimated the contribution of biomass burning based on K or K$^+$, a few studies had reported that K was not an ideal tracer for biomass burning, and it could be used as an appropriate biomass burning indicator only when most of K or K$^+$ was emitted from biomass burning. For example, Zhang *et al.* (2010) found that K$^+$ concentrations exhibited no apparent seasonal trends and it had poor correlation with fire counts in the

---

southeastern U.S. Minguillon *et al.* (2011) reported that K showed weaker correlation with EC from biomass burning under low concentration levels and also presented a background level of K in northeast Spain during wintertime. Wang *et al.* (2014) also found levoglucosan (a unique organic tracer for biomass burning) was highly correlated with OC ($R^2 = 0.80$) but not with K^+ ($R^2 = 0.36$) in Beijing. In order to have a better and more accurate estimate, some studies used the modified K concentration as a biomass burning source tracer in receptor models. For example, Pachon *et al.* (2013) defined biomass burning K as the difference between total K and dust source K in their PMF analysis.

However, there has been no study that is specifically designed to investigate the uniqueness and applicability of K in tracing biomass burning as a source. This is especially true in China, where source apportionment research is being widely carried out in many cities for identifying major sources of haze. It is essential to study if K can be used as a tracer for biomass burning as some studies used total K as a biomass burning tracer in receptor model when K^+ data were not available or K was measured by X-ray fluorescence analysis (XRF) (Heo *et al.*, 2009; Dall'Osto *et al.*, 2013; Yu *et al.*, 2013; Zíková *et al.*, 2016).

In this study, K and K^+ in $PM_{2.5}$ have been measured in different seasons by the online instruments Xact 625 (Cooper Environmental Services LLC, USA) and In-situ Gas and Aerosol Composition (IGAC, Model S-611, Fortelice International Co., Ltd., Taiwan) with a 1-hour time resolution in Beijing. Therefore, the objectives of this study included (1) to investigate if K can be used as a sole tracer for biomass burning in Beijing, (2) to quantify the major source contributions to K in Beijing across the four seasons.

METHODS

Sampling Information

The field campaign was conducted on the rooftop of an eight-floor building (30 m above ground level) at an urban monitoring station (PKUERS, 39.99N, 116.3E) in Peking University (PKU), Beijing. The measurements of K were conducted during one month of each season, including autumn (October 2015), winter (January 2016), spring (March 2016), and summer (August–September 2016). For K^+, the measurements were performed along with K in two seasons (winter and spring). The sampling site was located in the northwestern urban area of Beijing without obvious K sources nearby. The PKU campus is located in the residential and commercial area, which is representative of a typical urban site in Beijing (Wu *et al.*, 2008; Lin *et al.*, 2009). $PM_{2.5}$ mass concentration was measured by a tapered element oscillating microbalance (TEOM).

Online K Measured by an Xact 625

The online Xact 625 multi-metal monitor, which measured multiple metals continuously based on a XRF technique, has become a major tool in air quality monitoring in China. The Xact 625 can provide information on about twenty-three metals with a 1-hour time resolution, including K,

Ca, V, Cr, Cu, Zn, Ga, As, Mn, Fe, Co, Ni, Se, Ag, Cd, Sn, Sb, Au, Hg, Ba, Tl, Pb and Bi. With the Xact, ambient air was sampled on a Teflon filter tape through a $PM_{2.5}$ cyclone inlet at a constant flow rate of 16.7 L min^{-1}. Then the sample was automatically analyzed by nondestructive energy-dispersive X-ray fluorescence to determine the mass of metals. The Xact has been documented with Environment Technology Verification (ETV) and certified by the US Environment Protection Agency (USEPA, 2012). In addition, Zhou *et al.* (2017a) reported that K, Fe, Zn, Pb, Mn, Cu, Cr, Se, and Ni presented good correlations between online measurements by the Xact 625 and offline measurements by inductively coupled plasma mass spectrometry (ICP-MS).

For quality assurance (QA) and quality control (QC) of the Xact, a gas tightness test, flow calibration, blank filter test, and metal core sampler test as well as a standard filter calibration were conducted before operation of the instrument. Moreover, after each 1-h sample, a Pd rod was analyzed as part of an automatic internal quality control to check the stability of the instrument. The energy calibration test and energy level test were performed at a specific time each day (half hour after midnight) to monitor any possible shift of the Xact. More detailed information about the Xact 625 can be found in Gao *et al.* (2016), Chang *et al.* (2017), and Phillips-Smith *et al.* (2017).

Online K^+ Measured by an IGAC

Water-soluble K^+ was measured by an IGAC. Both gases and fine particles were collected by the system and selected gaseous and water-soluble ions were measured at a 1-h time resolution, including NH_4^+, Na^+, K^+, Ca^{2+}, Mg^{2+}, SO_4^{2-}, NO_3^-, and Cl^-. With the IGAC system, ambient air was drawn through a PM_{10} inlet followed by a $PM_{2.5}$ cyclone at a flow rate of 16.7 L min^{-1}, and then gas- and particle-phase samples were collected into an aqueous solution through a Wet Annular Denuder (WAD) and a scrub and Impact Aerosol Collector (SCI), respectively. Finally, samples were analyzed by ion chromatography (Dionex ICS-3000) for anions and cations. LiBr (0.14 ppm) was used as the internal standard and was added continuously to the SCI impaction plate at a flow rate of 0.1 mL min^{-1} along with each sample to ensure the stability of IC analysis. More information about the IGAC can be found in Young *et al.* (2016).

RESULTS AND DISCUSSION

Seasonal Variation of K and K^+ in Beijing

During the sampling period, based on the hourly data, the mass concentration of K varied from 101 to 6394 ng m^{-3}, with an average of 1016 ± 1019 ng m^{-3} (one standard deviation), and the mass concentration of K^+ varied from 94 to 6386 ng m^{-3}, with an average of 867 ± 1052 ng m^{-3}. The highest K concentration was found in spring (1355 ± 1194 ng m^{-3}), followed by winter and autumn, with the lowest in summer (492 ± 244 ng m^{-3}). K^+ was only measured in the winter and spring, with the average concentrations of 888 ± 1087 ng m^{-3} and 841 ± 1007 ng m^{-3}, respectively.

The time series of $PM_{2.5}$ K across the four seasons measured by the Xact 625 and $PM_{2.5}$ K^+ for winter and spring measured by the IGAC were shown in Fig. 1. It can be seen that the peak concentrations of K in autumn, winter and spring were in the range of 3000 to 6000 ng m^{-3}. However, the peak concentration of K was only about 900 ng m^{-3} during summer, which might be attributed to more precipitation, lower emissions and favorable meteorological conditions. Active biomass burning usually occurs in summer and autumn, which is mainly associated with crop harvesting followed by the burning of crop residuals. The highest fire counts were found in June (about 37% of total fires), followed by early October in northern China (Huang *et al.*, 2012; Yan *et al.*, 2017). However, higher concentrations of K were found in spring and winter than in autumn and summer. It should be noted that the lowest concentrations of K were almost similar for the four seasons (in the range of 170–230 ng m^{-3}), indicating similar background concentrations for the different seasons. In addition, during winter and spring, K and K^+ showed almost the same concentration levels and trends, suggesting that they might be affected by similar major sources.

Table 1 presented the comparison of K and K^+ concentrations in this study with those reported in previous studies in Beijing and other cities. It can be seen that K and K^+ concentrations were comparable among the different studies in Beijing (Zhang *et al.*, 2013a; Gao *et al.*, 2016; Li *et al.*, 2017). Compared with other cities in China, the concentration of K in Beijing is higher than that in Shanghai (Chang *et al.*, 2017) but lower than that in Chengdu (Tao *et al.*, 2014). As for K^+, the concentration in this study was higher than that in Guangzhou (Tao *et al.*, 2017) and lower than that in Chengdu (Tao *et al.*, 2014). Compared with other countries, the average concentration of K in Beijing was about one order of magnitude higher than those measured in the U.S. and Europe, while about two times higher than that in Korea. The percentages of K in measured metals in this study (including K, Fe, Ca, Zn, Pb, Ba, Mn, Cu, As, Cr, Se and Ni) in Beijing and the other cities were shown in Fig. S1. In China, K accounted for about 30–50% of the measured metals, higher than that in the U.S. and European cities (10–30%). This suggested K not only exhibited higher concentrations in China, but also contributed a higher percentage to the total metals. Therefore, it is very important to investigate K sources in Beijing.

Potential Sources of Atmospheric K in Beijing
Ambient K/K^+ and $K^+/PM_{2.5}$ Ratio Comparisons to Source Profiles

The K/K^+ ratio could be used to distinguish sources of K to some extent. Previous studies have reported a high ratio of K/K^+ for dust (about 3.93-8.27) (Shen *et al.*, 2016; KLACP, 2017), but a low ratio for biomass burning emissions (about 1.17–2.01) (Tian, 2016; KLACP, 2017). In addition, the $K^+/PM_{2.5}$ ratios can also vary with sources. K^+ accounted for about 2–5% of $PM_{2.5}$ in biomass burning, about 0.2–2.7% of $PM_{2.5}$ in coal combustion (Wang *et al.*, 2009; Wang, 2016; KLACP, 2017), but only 0.1–0.3% in dust (Shen *et al.*, 2016; Tian, 2016; KLACP, 2017). Therefore, using the ratios of K/K^+ and $K^+/PM_{2.5}$ could help to distinguish K sources, and these ratios in various source profiles were given in Table S1.

The relationships between K and water-soluble K^+ during spring and winter were examined in Fig. 2 under different $PM_{2.5}$ concentrations ($PM_{2.5} < 35$ µg m^{-3}, $35 < PM_{2.5} < 150$ µg m^{-3} and $PM_{2.5} > 150$ µg m^{-3}, representing clean, light pollution and heavy pollution periods, respectively). K and K^+ showed good correlations for all cases with the r^2 values ranging from 0.82 to 0.96 in spring and 0.72 to 0.77 in winter, suggesting that K and K^+ had similar emission sources. During our study period, a severe dust storm episode was observed in spring, with extremely high Ca concentrations (> 8000 ng m^{-3}) and high wind speed (> 6 m s^{-1}). However, during this dust episode K and K^+ showed a poor correlation ($r^2 = 0.35$) (Fig. 2((a-4)). In addition, the K/K^+ ratio in the ambient samples during the spring dust period was the same as that in the dust source profile (KLACP, 2017).

Fig. 3 presented ratios of $K^+/PM_{2.5}$ and K/K^+ in the different seasons during this study and those from different sources (e.g., cooking, biomass burning, coal combustion, and dust). As Fig. 2 showed, the K/K^+ ratio decreased when $PM_{2.5}$ concentration increased, suggesting more influence from biomass burning, residential coal burning, and coal-fired boilers as the K/K^+ ratio in ambient $PM_{2.5}$ samples are similar to that in these sources. This implied that when the concentration of $PM_{2.5}$ was high during haze episodes, coal combustion contributed more to K in ambient aerosol in Beijing. Coal combustion was a unique source of air pollution in China compared to Europe and the U.S., and residential coal combustion was proved to contribute to haze during cold seasons in Beijing in recent years, because of
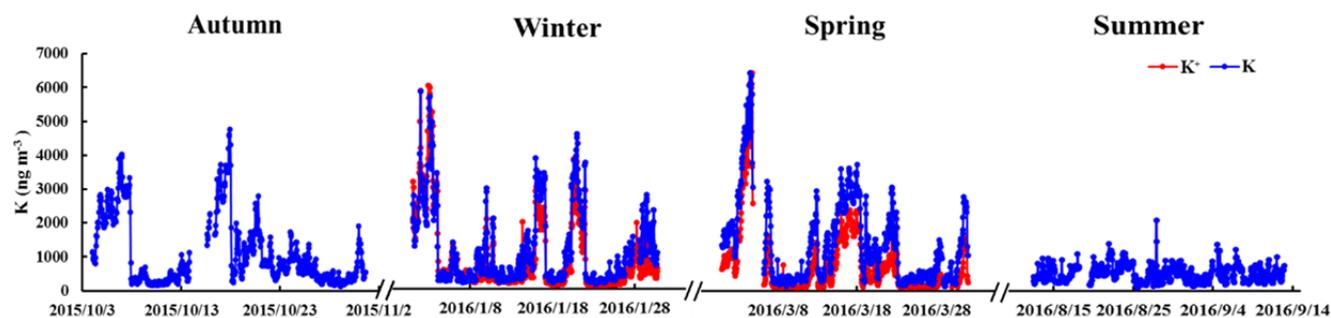

Fig. 1. Time series of K and K^+ concentrations with an 1-hour time resolution across the study period.

Table 1. Comparison of K and K$^+$ concentrations with other studies.

| City	Season	Measurement Method	K (ng m^{-3})	K$^+$ (ng m^{-3})	K/PM$_{2.5}$	K$^+$/PM$_{2.5}$	Reference
Beijing	Autumn (2015/10)	Xact 625, IGAC	1100 ± 998	888 ± 1087	2.02 ± 1.44%	1.91 ± 1.82%	This study
	Winter (2016/1)		1117 ± 1113	841 ± 1007	2.40 ± 1.86%	1.03 ± 1.12%	
	Spring (2016/3)		1355 ± 1194		1.66 ± 1.33%		
	Summer (2016/8)		492 ± 244		1.82 ± 1.20%		
Beijing	Summer (2014/8)	Xact 625	713 ± 407		1.15 ± 1.03%		Gao et al., 2016
Beijing	2014	Online XRF	900 ± 2300		1.11 ± 3.01%		Li et al., 2017
Beijing	Winter (2013/1)	Online IC (URG)		1380			Han et al., 2016
Beijing	Spring (2009/4)	Filter_IC		1080 ± 710		0.86 ± 1.20%	Zhang et al., 2013
	Summer (2009/7)			660 ± 470		0.48 ± 0.98%	
	Autumn (2009/10)			1130 ± 900		0.84 ± 1.64%	
	Winter (2010/1)			810 ± 770		0.58 ± 0.89%	
Shanghai	2016	Xact 625	388.6				Chang et al., 2017
Guangzhou	Spring (2014/4)	Filter_IC		600 ± 300		1.36 ± 1.67%	Tao et al., 2017
	Summer (2014/6)			500 ± 300		1.35 ± 1.87%	
	Autumn (2014/10)			600 ± 300		1.25 ± 1.76%	
	Winter (2014/12)			1000 ± 700		1.58 ± 2.50%	
Chengdu	Spring (2011/3)	Filter_ICP-MS, IC	1575 ± 751	1500 ± 800	1.25 ± 1.32%	1.19 ± 1.21%	Tao et al., 2014
	Summer (2011/7)		1312 ± 623	1300 ± 600	1.47 ± 1.78%	1.46 ± 1.71%	
	Autumn (2011/10)		1757 ± 777	1800 ± 700	1.58 ± 1.58%	1.62 ± 1.42%	
	Winter (2011/1)		1681 ± 640	2100 ± 700	1.06 ± 1.25%	1.32 ± 1.37%	
Taiwan	2011	Filter_ICP-MS	141		0.65%		Gugamsetty et al., 2012
Seoul, Korea	2003–2006	Filter_PIXE	409		0.94%		Heo et al., 2009
New Delhi, India	Summer (2014/7)	Filter_IC		860 ± 490		1.47 ± 1.40%	Pant et al., 2015
	Winter (2013/12)			3830 ± 1630		1.38 ± 1.63%	
Barcelona, Spain	2011	Filter_ICP-AES	128		0.69%		Salameh et al., 2015
Marseille, France		Filter_ICP-MS	225		1.15%		
Genoa, Italy		Filter_XRF	100		0.71%		
California, US	2001	Filter_XRF	122		0.29%		Na et al., 2009
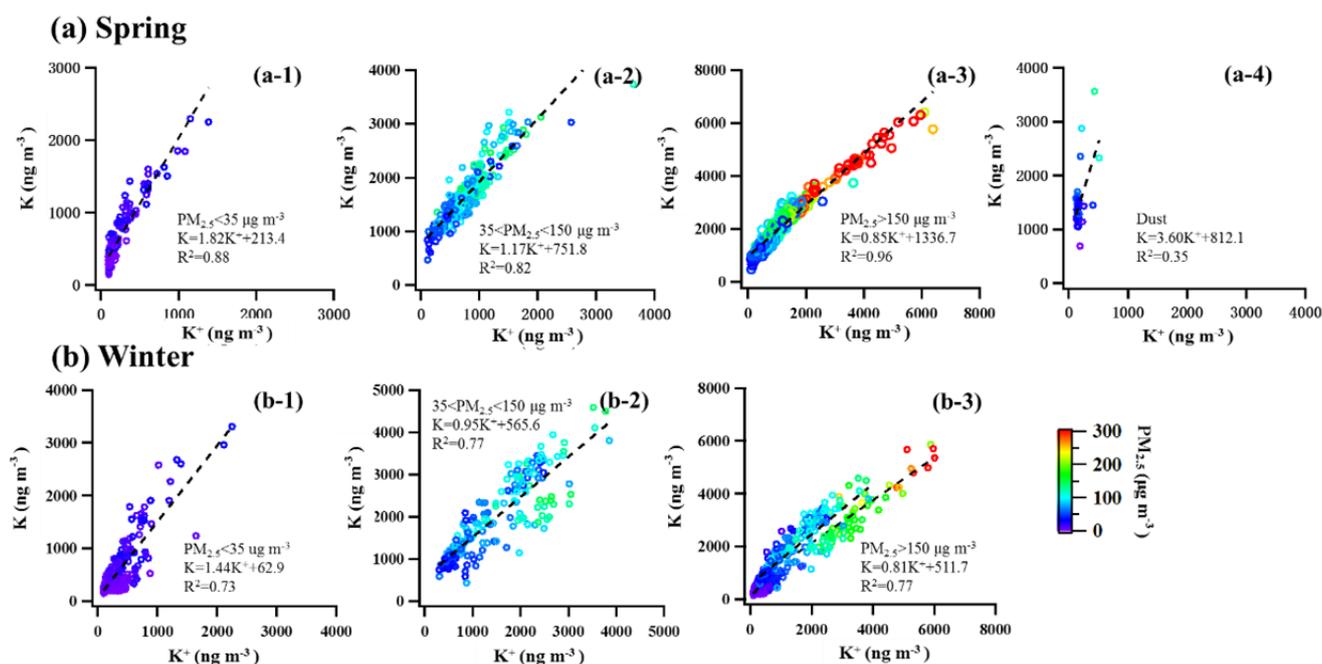
Fig. 2. The correlations between K and K^+ in Beijing in spring (a) and winter (b) colored by the $PM_{2.5}$ concentration. (a-1) to (a-3) represent the correlations during clean ($PM_{2.5} < 35$ μg m^{-3}), light pollution ($35 < PM_{2.5} < 150$ μg m^{-3}) and heavy pollution ($PM_{2.5} > 150$ μg m^{-3}) periods in spring, and (b-1) to (b-3) represent the same periods in winter. (a-4) represented a typical dust event in spring.
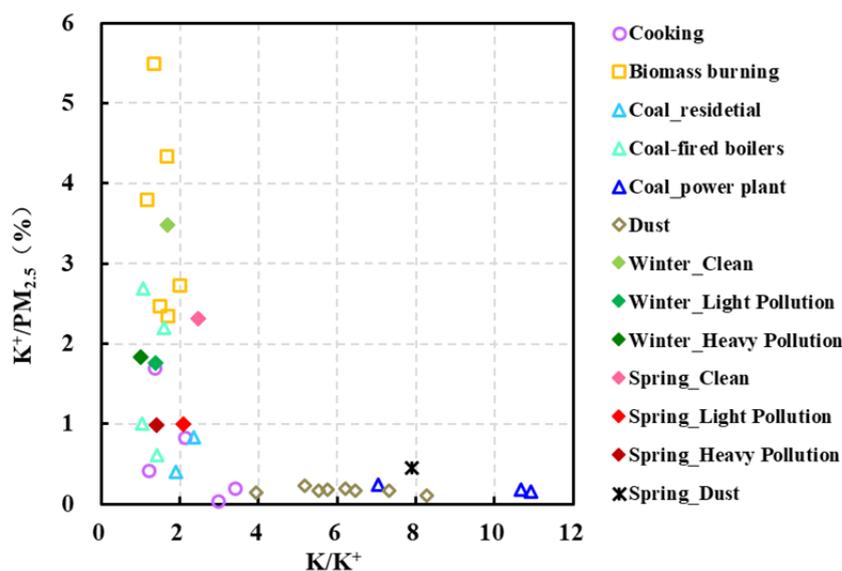

Fig. 3. Scatter plots of $K^+/PM_{2.5}$ versus K/K^+ from different literature source profiles as well as ambient samples (spring and winter) in this study. $PM_{2.5}$ pollution levels: clean ($PM_{2.5} < 35$ μg m^{-3}), light pollution ($35 < PM_{2.5} < 150$ μg m^{-3}), and heavy pollution ($PM_{2.5} > 150$ μg m^{-3}). The references for the profiles are as follows, cooking (Zhang *et al.*, 2016, 2017), biomass burning (Tian, 2016; KLACP, 2017), residential coal (KLACP, 2017), coal_bolier (Wang *et al.*, 2009; KLACP, 2017), coal_power plant (Wang, 2016), and dust (Shen *et al.*, 2016; KLACP, 2017).

its low combustion efficiency and lack of flue gas treatment devices in the rural areas of Beijing and its adjacent provinces (Liu *et al.*, 2016, 2017).

As mentioned above, the highest K/K^+ ratio was found in the clean periods, suggesting that K in clean days was more influenced by dust or cooking sources. This corresponded well with the fact that the lowest $PM_{2.5}$ concentration in Beijing was often found under strong northwest winds. Therefore, during those days, strong winds could lead to high dust and local source contributions such as cooking could also dominate in K sources.

Correlation between K and Coal Combustion Source Tracers

It can be seen in Table 2 that K exhibited strong correlations (r > 0.8) with Pb, Se, As, Zn, and Mn in autumn, winter and spring, but relatively weaker correlations in summer. K^+ also showed strong correlations with those metals in winter and spring. In previous studies, Pb, As, and Se have been used as markers for coal combustion (Song *et al.*, 2006; Yu *et al.*, 2013; Gao *et al.*, 2016). According to the emission inventory, coal combustion was a dominant contributor to particulate Pb, As, Se, Mn, Hg and Co in China (Tian *et al.*, 2010, 2015). Therefore, the strong correlations between K (and K^+) and Pb, As, Se, Zn and Mn suggested that coal combustion could be an important source to K in Beijing.

K and K^+ did not show strong correlations with Ca in this study. Ca, Al and Ba were usually used as tracers for dust (Song *et al.*, 2006; Yu *et al.*, 2013; Gao *et al.*, 2016; Zíková *et al.*, 2016). Thus, the weak correlations suggested that dust might not be a major source of K in Beijing although it was relatively more important in clean days or during spring dust episodes. Both K and K^+ had good correlations with $PM_{2.5}$ across the four seasons, especially for K in autumn (r = 0.92). In order to check whether synoptic meteorology is an important factor in leading to the good correlation between K, K^+ and $PM_{2.5}$, a correlation analysis between $PM_{2.5}$ and all metal species measured was shown in Table S2. It can be seen in Table S2 that $PM_{2.5}$ did not show good correlation with all metal species, including Ca, Ba, Cr, Ni, suggesting that $PM_{2.5}$ pollution was related to sources that contributed to K.

Source Apportionment of Atmospheric K in Beijing

Based on the above analyses of K/K^+ ratios and the correlations between K and coal tracers, it was observed that coal combustion was also an important source of K in Beijing, in addition to biomass burning and dust. Furthermore, since Beijing is not a coastal city, the source

contribution of K from sea salt can be ignored. Thus, the contributions of these three sources (dust, coal combustion, and biomass burning), will be quantified using source specific ratios in the following discussion.

The K/Ca Ratio for Dust

Dust can have different types including soil dust, road dust, construction dust, and mineral dust from the desert (Zhang *et al.*, 2014; Shen *et al.*, 2016). Several studies have applied the ratios of dust tracer species (Ca, Fe, Al, Si, and so on) and K to estimate the fraction of dust-K, based on the hypothesis that the tracer species were uniquely emitted from dust source and had relative stable ratios with K. For example, Lewis *et al.* (2003) used a K/Si ratio of 0.15 and Pio *et al.* (2008) used a K/Ca ratio of 0.12, which was consistent with the ratios in soil. Pachon *et al.* (2013) used a K/Fe ratio of 0.37, which was obtained by the linear regression of K and Fe from long-term measurement data. Considering that Fe in ambient aerosol in Beijing could be partly from metal smelting sources transported from neighboring provinces such as Hebei, Ca was selected as the most suitable tracer for dust in this study.

The percentage of K and Ca in $PM_{2.5}$ and the ratio of K/Ca from the source profiles of different dust sources were summarized in Table 3. It can be seen that the emissions from road dust and construction dust were enriched in Ca (accounting for about 3.5–29.1% in $PM_{2.5}$) compared with those from desert and Gobi dust (1.4–3.9% in $PM_{2.5}$). In contrast, desert and Gobi dust were relatively enriched with K (1.5–3.0% in $PM_{2.5}$) compared with road dust and construction dust (0.6–1.3% in $PM_{2.5}$, except for construction dust in Nanjing [4.0%]). Therefore, the ratios of K/Ca in desert and Gobi dust (about 0.72–1.03) were higher than road dust and construction dust (about 0.05–0.26).

Dust events are seasonal. Beijing is located in the downwind region for dust transport from Mongolia and Inner Mongolia. Northwest dust will hit Beijing under suitable weather systems, and mainly occur in spring

Table 2. Pearson correlations between K, K^+, and trace metals in $PM_{2.5}$.

	K_Autumn		K_Winter		K_Spring		K_Summer		K^+_Winter		K^+_Spring	
	r	n	r	n	r	n	r	n	r	n	r	n
$PM_{2.5}$	0.92**	592	0.83**	648	0.90**	621	0.77**	695	0.87**	642	0.86**	522
K	1.00**	611	1.00**	692	1.00**	728	1.00**	701	0.94**	685	0.95**	604
Pb	0.97**	611	0.93**	692	0.92**	728	0.79**	701	0.92**	685	0.88**	604
Zn	0.94**	611	0.92**	692	0.90**	728	0.68**	701	0.91**	685	0.85**	604
Fe	0.90**	611	0.93**	692	0.83**	728	0.80**	701	0.92**	685	0.65**	604
Mn	0.88**	611	0.86**	692	0.87**	728	0.74**	701	0.89**	685	0.79**	604
Cu	0.89**	611	0.77**	692	0.79**	728	0.62**	701	0.75**	685	0.70**	604
Ca	0.60**	611	0.63**	692	0.44**	728	0.39**	701	0.62**	685	0.17**	604
Ba	0.91**	611	0.78**	692	0.62**	728	0.75**	701	0.79**	685	0.36**	604
As	0.83**	397	0.81**	586	0.77**	551	0.51**	481	0.78**	580	0.82**	517
Cr	0.53**	472	0.56**	622	0.49**	574	0.21**	578	0.66**	615	0.45**	521
Se	0.96**	459	0.88**	671	0.95**	623	0.80**	603	0.88**	664	0.95**	555
Ni	0.72**	572	0.70**	678	0.86**	688	0.37**	644	0.69**	671	0.87**	582

** denotes correlation is significant at the 0.01 level.
"n" denotes the number of samples used in correlation analyses.
"r" denotes the correlation coefficient.

Table 3. The percent contributions of K and Ca to PM$_{2.5}$ as well as the K/Ca ratio for source profile of dust (road dust, construction dust, and desert dust).

Site_source type	K (%)	Ca (%)	K/Ca	Reference
Beijing_dust	2.85	6.23	0.46	This study
Beijing_road dust	0.94	3.92	0.24	KLACP, 2017
Beijing_road dust	0.91	3.55	0.26	
Beijing_road dust	1.02	7.04	0.14	
Beijing_construction dust	0.59	11.40	0.05	
Beijing_construction dust	1.18	15.23	0.08	
Beijing_construction dust	1.33	10.78	0.12	
Beijing_road dust	1.09	5.69	0.19	Shen et al., 2016
Beijing_construction dust	1.20	11.57	0.10	
Tianjin_road dust	1.03	4.30	0.24	
Tianjin_construction dust	1.22	7.88	0.16	
Nanjing_road dust	1.00	9.93	0.10	Fan, 2006
Nanjing_construction dust	4.01	29.05	0.14	
Taklimakan Desert	3.00	2.99	1.00	Zhang et al., 2014
Xinjiang Gobi	2.81	3.90	0.72	
Central Inner Mongolia Desert	1.49	1.44	1.03	

(Zhang *et al.*, 2007; Xu *et al.*, 2016). In addition, local construction dust and road dust can affect Beijing across all seasons because of traffic and wind. Thus, the mixed characteristics of local dust and northwest dust should be taken into consideration in the dust source K estimation for spring, but local dust should be considered for all other seasons.

In this study, a typical dust episode was observed in spring, as discussed in Section 3.2.1. During the dust episode (March 5, 2016), extremely high Ca concentrations (> 8000 ng m^{-3}) and high wind speeds (> 6 m s^{-1}) were observed. The ratio of PM$_{2.5}$/PM$_{10}$ rapidly decreased from 0.94 to 0.17 with an average ratio was 0.2 for the whole episode. The highest concentration of PM$_{10}$ reached 679 μg m^{-3} and the main pollutant in the atmosphere was PM$_{10}$. For non-dust episodes the concentration of Ca was relatively low (< 2000 ng m^{-3}), and the ratio of PM$_{2.5}$/PM$_{10}$ was usually higher than 0.50. A good correlation (r^2 = 0.96) between Ca and K during this dust episode suggested that they came from the same source, as shown in Fig. 4(a). Under non-dust cases (see Fig. 4(b)), Ca and K showed relatively weak correlation (r^2 = 0.40), suggesting K was mainly contributed by other sources than dust. The linear regression slope of K and Ca during this dust episode was 0.35, and the ratio of the average concentration of K/Ca was 0.46, which was within the range of K/Ca influenced by local dust (road dust and construction dust) and northwest dust (desert and Gobi dust). Therefore, this episode was most likely to be affected by both dust transported from the northwest region and local dust. Backward trajectories from the northwest direction, which is the source region for Mongolia and Inner Mongolia dust, also indicated that this dust episode was influenced by this region (Fig. S2). High wind speeds (> 6 m s^{-1}) during dust episodes could lead to high emissions of local road dust and construction dust as well. In the following calculation, the K/Ca ratio of 0.35 found in this episode was used as the source ratio of dust in spring. For the other seasons, the ratio of K/Ca was

0.15, which was obtained from the average ratio (0.15 ± 0.07) for the road dust and construction dust source profiles in Beijing (Table 3).

The K/Pb Ratio for Coal Combustion

As discussed in Section 3.1, coal combustion might be an important source of PM$_{2.5}$ K in Beijing. To our best knowledge, currently the contribution of coal combustion to PM$_{2.5}$ K is still not well understood. In this study, the ratios of K to tracers of coal combustion were applied to estimate the contribution of coal-K. It was observed that Pb and As, which were usually used as tracers of coal combustion, exhibited good correlations with K across the different seasons (see Table 2). In order to identify an appropriate ratio of K and source tracers to estimate the source contribution of coal combustion, the relationship between K, Pb and As were further investigated. The ratios of K/Pb and K/As under different PM$_{2.5}$ concentration levels across the four seasons were shown in Fig. 5 and Table S3. It was found that under the high PM$_{2.5}$ concentration levels (PM$_{2.5}$ > 90th percentiles, Fig. 5) the ratios of K/Pb and K/As were more stable (K/Pb: 15.70 ± 3.57 and K/As: 64.43 ± 20.47) compared to those under other PM$_{2.5}$ concentration levels (PM$_{2.5}$ < 10th percentiles and 10th < PM$_{2.5}$ < 90th percentiles, K/Pb: 24.20 ± 18.25, K/As: 130.47 ± 93.01) across the four seasons, suggesting the influence of a homogeneous source under high PM$_{2.5}$ concentration levels.

Compared to K/As, the ratio of K/Pb was more suitable for estimating coal combustion because it exhibited a more stable value during the sampling period. The ratios of K/As showed relatively large variations, which might be attributed to the low concentration of PM$_{2.5}$ As, even lower than the method detection limits (0.114 ng m^{-3}) in some cases. A slight change of As concentration will result in a large variation in the K/As ratios. Moreover, online-Pb measured by the Xact 625 correlated well with offline-Pb measured by ICP-MS (slope = 1.03, R^2 = 0.98), while As
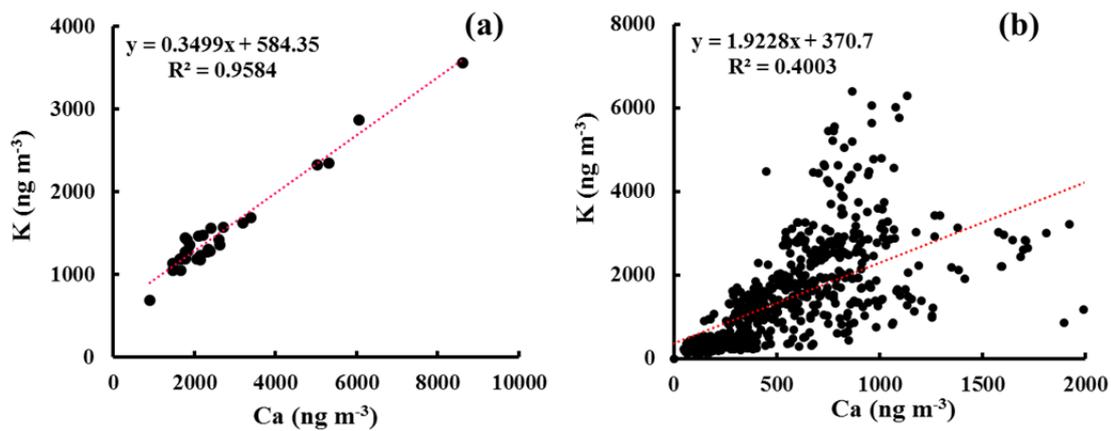
Fig. 4. The correlation between K and Ca during (a) dust and (b) non-dust periods in spring.
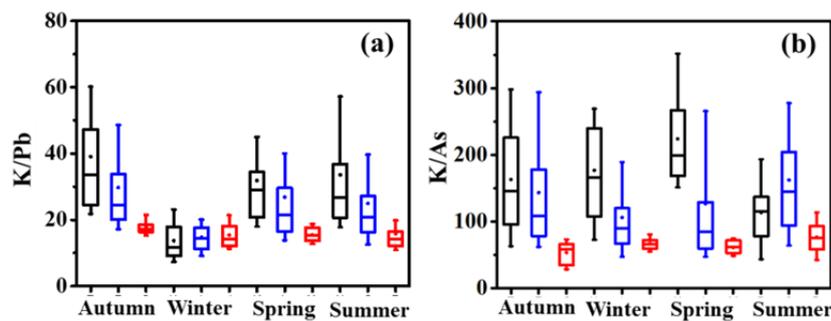

Fig. 5. The ratios of (a) K/Pb and (b) K/As across the four seasons. Color bars represented different $PM_{2.5}$ concentration levels: black, blue and red represented $PM_{2.5}$ < 10th percentiles, 10th < $PM_{2.5}$ < 90th percentiles, and $PM_{2.5}$ > 90th percentiles, respectively.

exhibited a bad correlation between online and offline measurements (slope = 5.53, R^2 = 0.14) (Zhou *et al.*, 2017a). Several studies have reported that the major sources of Pb in Beijing were coal combustion and industry after leaded gasoline was phased out in 1997. The transportation contribution of the surrounding areas was another important source (Sun *et al.*, 2006; Cai *et al.*, 2017). According to the emissions inventory of Pb, coal combustion contributed more than 50% to atmospheric Pb in China (Li *et al.*, 2012; Tian *et al.*, 2015), and about 70% of atmospheric Pb emissions in Beijing were from coal combustion in 2009 and 2010 (Cai *et al.*, 2017). Thus, Pb was a suitable tracer for coal combustion in this study.

Moreover, the ratios of K/Pb under any $PM_{2.5}$ concentration levels in winter also showed relatively stable values compared with the other seasons (see Table S2), and was very similar to that during high $PM_{2.5}$ concentration periods, which might be attributed to more coal combustion in winter. Besides, the ratio of K/Pb (15.70 ± 3.57) under high $PM_{2.5}$ concentration levels was comparable to that found in the coal combustion source profile (10.58) (Ma *et al.*, 2015). It is also close to that observed in Wangdu (12.43) (a suburban site in Hebei Province, in the southwest of Beijing, about 170 km away from Beijing) (Zhou *et al.*, 2017b) and Baoding (8.75) (an industrial city in Hebei Province, in the southwest of Beijing, about 140 km away from Beijing) (Liu *et al.*, 2017), where coal combustion

was a significant source of $PM_{2.5}$. Therefore, it is clear that coal combustion was one of the major sources of K in $PM_{2.5}$, especially during severe haze periods.

The stable ratio of K/Pb (15.70) obtained from ambient measurement under high $PM_{2.5}$ concentration levels in this study could well represent the characteristics of K and Pb from local coal combustion. This ratio could be used to estimate the contribution of coal combustion to atmospheric K.

Source Contribution of Atmospheric K

Based on the hypothesis that source specific species were unique from dust or coal combustion source emissions and had relatively stable ratios with K, the contributions of dust and coal combustion to K could be roughly estimated. Then, K from biomass burning ($K_{Biomass\ burning}$) could be defined as the fraction of total K (K_{Total}) apart from K from dust (K_{Dust}) and coal combustion (K_{Coal}). As discussed above, Ca and Pb were selected as appropriate source indicators for dust and coal combustion, respectively. The ratios of K/Ca used were 0.35 for spring and 0.15 for other seasons in Eq. (1) and K/Pb (15.70) in Eq. (2) to estimate K_{Dust} and K_{Coal}. Then $K_{Biomass\ burning}$ was estimated based on Eq. (3). Considering about 70% of Pb was emitted from coal combustion in Beijing (Tian *et al.*, 2015; Cai *et al.*, 2017), the concentration of Pb was multiplied by 0.7 in Eq. (2) to estimate K from coal combustion.

$$K_{Dust,i} \text{ (ng m}^{-3}) = K/Ca \times Ca_i \text{ (ng m}^{-3}) \tag{1}$$

$$K_{Coal,i} \text{ (ng m}^{-3}) = K/Pb \times Pb_i \text{(ng m}^{-3}) \times 0.7 \tag{2}$$

$$K_{Biomass\ burning,i} \text{ (ng m}^{-3}) = K_{Total,i} \text{ (ng m}^{-3}) - K_{Dust,i} \text{ (ng m}^{-3}) - K_{Coal,i} \text{ (ng m}^{-3}) \tag{3}$$

where the i subscript represents the ith sample, time resolution for each sample was an hour in this study. For most of the sampling period, K_{Dust}, K_{Coal} and $K_{Biomass\ burning}$ were all higher than zero, indicating these three sources all have contributions to $PM_{2.5}$ K. However, sometimes the sum of K_{Dust} and K_{Coal} exceeded total K. In this case, the fraction of K from biomass burning was defined as zero. The underestimation of biomass burning source contribution was infrequent and was only observed when the concentration of $PM_{2.5}$ was very low (e.g., $PM_{2.5} < 10$ µg m^{-3}). Under these conditions, the fraction of Pb from coal emission in Beijing (70%) might be over-evaluated, thus resulting in overestimated coal combustion contributions to K. That is, the estimation method in this study was suitable for most sampling periods, especially for heavy pollution episodes, but not applicable for very clean period ($PM_{2.5} < 10$ µg m^{-3}) when the contribution of biomass burning to K might be underestimated.

The average source contributions of dust, coal combustion and biomass burning to K across the four seasons were plotted in Fig. 6(a). It was clear that coal combustion had the largest contribution (45–69%) to atmospheric K in Beijing. However, biomass burning and coal combustion showed similar source contributions in autumn, accounting for 49% and 45%, respectively. The high coal combustion contribution (69%) to K in winter might be primarily associated with the increased residential coal combustion for heating, while its contributions (45–52%) during the non-heating seasons (e.g., summer, autumn, and spring) could be attributed to industrial coal combustion and/or the transportation from surrounding areas. This result was consistent with the above analysis, that $PM_{2.5}$ K was largely affected by coal combustion sources in Beijing. Biomass burning contributed about 26–49% of atmospheric K, suggesting it was not the dominant source of atmospheric K in Beijing. This result corresponded well to the finding of Wang *et al.* (2014), which reported that the fractions of K^+ from biomass burning were about 44 ± 26% and 33 ± 30% in total K^+ in autumn and spring respectively. However, the contribution of biomass burning could reach as high as 49% in autumn, much higher than the other seasons. This was mainly because autumn is the harvest season and agricultural waste open burning activities occur frequently. Additionally, the contribution of dust was the highest in spring (19%), higher than that in summer (9%), autumn (6%) and winter (5%).

The time series of absolute and relative contributions of each source to atmospheric K across the four seasons in Beijing were presented in Figs. 6(b) and 6(c). Coal combustion was the primary source in winter, contributing 50–90% of K, and biomass burning and dust contributed
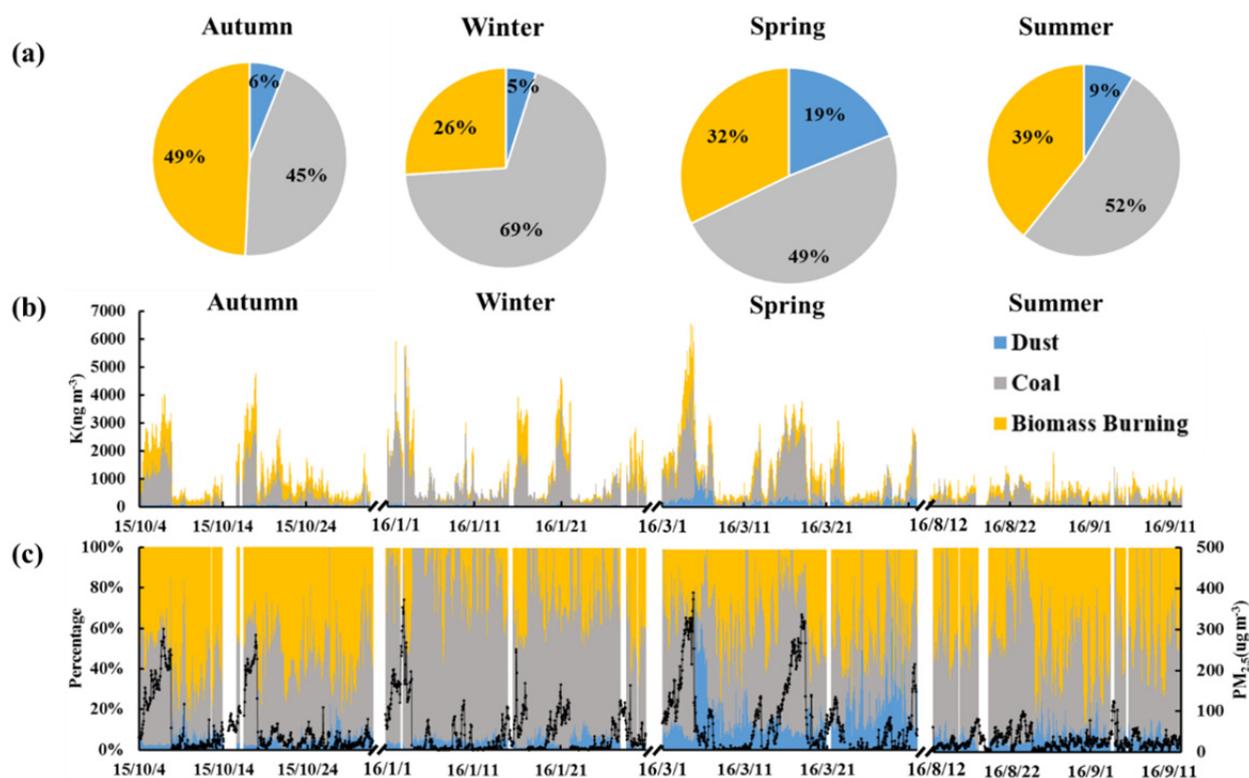

Fig. 6. (a) Average source contribution, (b) time series of mass concentration of K, and (c) time series of mass fractions of dust, coal combustion and biomass burning to K along with the total $PM_{2.5}$ concentration across the four seasons. The size of each pie is proportional to the average concentration of K during that season.

Table 4. The average contributions (one standard deviation) of dust, coal combustion and biomass burning to K across the different seasons and the uncertainties.

	Dust		Coal		Biomass burning	
	contributions	Unc.	contributions	Unc.	contributions	Unc.
Autumn	6 ± 4%	3%	45 ± 17%	10%	49 ± 16%	11%
Winter	5 ± 4%	2%	69 ± 14%	20%	26 ± 15%	20%
Spring	19 ± 14%	4%	50 ± 20%	12%	33 ± 17%	13%
Summer	9 ± 5%	4%	54 ± 21%	13%	40 ± 18%	14%

"Unc. " denotes the uncertainties of source contributions.

less (less than 30%). In autumn, biomass burning dominated the K emissions and accounted for more than 50% in many cases. During the dust episode in spring, dust played an important role in atmospheric K, which contributed about 50–70%. However, under high $PM_{2.5}$ concentration levels, coal combustion became the predominant source, contributing more than 80% of total K, especially in winter. Overall, this implied there would be an overestimation of biomass burning if K were used as a sole tracer for biomass burning in the receptor model at such conditions.

Uncertainty Analysis

It is necessary to analyze the potential uncertainty in the estimation method for the different source contributions. According to the calculation method for different source contributions, a detailed uncertainty analysis was performed with consideration to two aspects: (1) The measurement uncertainty by Xact instrument. The 5/6 method detection limits (MDL) of K, Ca, and Pb were used as uncertainties of measuring concentrations (MDL: K: 2.37 ng m^{-3}, Ca: 0.90 ng m^{-3} and Pb: 0.22 ng m^{-3}). (2) The uncertainties of elemental ratios (K/Ca, K/Pb). Based on the dust source profiles in Beijing (Table 3), ranges of K/Ca ratio (0.05–0.26) was considered, and the standard deviation of K/Ca (0.07) was used as its uncertainty. And for K/Pb ratio, the relative stable ratio (15.70 ± 3.57) during high pollution episodes in this study was used to estimate coal combustion contribution, and the standard deviation (3.57) was used as the uncertainty of K/Pb. Then, the uncertainties of different source contributions were calculated based on propagation of uncertainty. More details about the uncertainty calculation process were listed in supplementary materials.

The average source contributions to K across the different seasons were shown in Table 4. It can be concluded that the uncertainty for the estimation of biomass burning and coal combustion were about 10–20%, for the dust contribution was 2–4% and the uncertainties were the greatest in winter.

CONCLUSIONS

The concentrations of K and water-soluble K$^+$ in $PM_{2.5}$ were observed by the Xact and IGAC with a 1-hour time resolution across the different seasons in Beijing. Sources of atmospheric K in the $PM_{2.5}$ in Beijing were investigated from both qualitative and quantitative perspectives. It was found that the ratios of K/K$^+$ and K/$PM_{2.5}$ were close to that of coal combustion source ratios and that K exhibited good correlations with coal combustion related trace

metals (e.g., Pb, As, Se, Zn, and Mn), suggesting that coal combustion was a major source of atmospheric K in Beijing. Source specific ratios of K/Pb (indicating a coal combustion source) and K/Ca (indicating a dust source) were applied to apportion the contributions of K from dust, coal combustion, and biomass burning. The results showed that the major source of K was coal combustion, which contributed about 45–69% of the K in Beijing, followed by biomass burning and dust. However, it exhibited a seasonality effect, with the largest source being coal combustion in winter (69%), biomass burning in autumn (49%), and dust in spring (19%). Furthermore, coal combustion was the predominant source during haze episodes, contributing more than 80% of the total K. It is clear that using K as a sole tracer for biomass burning results in an overestimation of the contribution of the latter, especially during winter haze episodes. Thus, our study indicates that K should not be used as a sole tracer for biomass burning in Beijing.

SUPPLEMENTARY MATERIAL

Supplementary data associated with this article can be found in the online version at http://www.aaqr.org.

REFERENCE

Andreae, M.O. (1983). Soot carbon and excess fine potassium-long-range transport of combustion-derived aerosols. *Science* 220: 1148–1151.

Cai, J., Wang, J.D., Zhang, Y.J., Tian, H.Z., Zhu, C.Y., Gross, D.S., Hu, M., Hao, J.M., He, K.B., Wang, S.X. and Zheng, M. (2017). Source apportionment of Pb-containing particles in Beijing during January 2013. *Environ. Pollut.* 226: 30–40.

Chang, Y.H., Huang, K., Deng, C.R., Zou, Z., Liu, S.D. and Zhang, Y.L. (2017). First long-term and near real-time measurement of atmospheric trace elements in Shanghai,

China. *Atmos. Chem. Phys. Discuss., in Review.*

Dall'Osto, M., Querol, X., Amato, F., Karanasiou, A., Lucarelli, F., Nava, S., Calzolai, G. and Chiari, M. (2013). Hourly elemental concentrations in PM$_{2.5}$ aerosols sampled simultaneously at urban background and road site during SAPUSS – diurnal variations and PMF receptor modelling. *Atmos. Chem. Phys.* 13: 4375–4392.

Duan, F.K., Liu, X.D., Yu, T. and Cachier, H. (2004). Identification and estimate of biomass burning contribution to the urban aerosol organic carbon concentrations in Beijing. *Atmos. Environ.* 38: 1275–1282.

Duvall, R.M., Majestic, B.J., Shafer, M.M., Chuang, P.Y., Simoneit, B.R.T. and Schauer, J.J. (2008). The water-soluble fraction of carbon, sulfur and crustal elements in Asian aerosols and Asian soils. *Atmos. Environ.* 42: 5872–5884.

USEPA (2012). *Environmental technology verification report: Pall corporation Xact 625 particulate metals monitor.* US EPA, Office of Research and Development, EPA/600/R-12/680.

Fan, S.X. (2006). *Comparative researches on PM$_{2.5}$ and PAHs compositions between urban and suburb in Nanjing.* Nanjing University of Information Science and Technology, China. (in Chinese)

Gao, J., Peng, X., Chen, G., Xu, J., Shi, G.L., Zhang, Y.C. and Feng, Y.C. (2016). Insights into the chemical characterization and sources of PM$_{2.5}$ in Beijing at a 1-h time resolution. *Sci. Total Environ.* 542: 162–171.

Gugamsetty, B., Wei, H., Liu, C.H., Awasthi, A., Hsu, S.C., Tsai, C.J., Roam, G.D., Wu, Y.C. and Chen, C.F. (2012). Source characterization and apportionment of PM$_{10}$, PM$_{2.5}$ and PM$_{0.1}$ by using positive matrix factorization. *Aerosol Air Qual. Res.* 12: 476–491.

Han, B., Zhang, R., Yang, W., Bai, Z.P., Ma, Z.Q. and Zhang, W.J. (2016). Heavy haze episodes in Beijing during January 2013: Inorganic ion chemistry and source analysis using highly time-resolved measurements from an urban site. *Sci. Total Environ.* 544: 319–329.

Heo, J.B., Hopke, P.K. and Yi, S.M. (2009). Source apportionment of PM$_{2.5}$ in Seoul, Korea. *Atmos. Chem. Phys.* 9: 4957–4971.

Huang, X., Li, M.M., Li, J.F. and Song, Y. (2012). A high-resolution emission inventory of crop burning in fields in China based on MODIS Thermal Anomalies/Fire products. *Atmos. Environ.* 50: 9–15.

KLACP (Key Laboratory of Aerosol Chemistry and Physics, Chinese Academy of Sciences) (2017). PM$_{2.5}$ main source profiles database in China, http://www.sourceprofile.org.cn/.

Lawson, D.R. and Winchester, J.W. (1979). Sulfur, potassium and phosphorus associations in aerosols from South-American Tropical Rain forests. *J. Geophys. Res.* 84: 3723–3727.

Lewis, C.W., Norris, G.A., Conner, T.L. and Henry, R.C. (2003). Source apportionment of phoenix PM$_{2.5}$ aerosol with the unmix receptor model. *J. Air Waste Manage. Assoc.* 53: 325–338.

Li, J., Pósfai, M., Hobbs, P.V. and Buseck, P.R. (2003). Individual aerosol particles from biomass burning in southern Africa: 2, Compositions and aging of inorganic particles. *J. Geophys. Res.* 108: 347–362.

Li, Q., Cheng, H.G., Zhou, T., Lin, C.Y. and Guo, S. (2012). The estimated atmospheric lead emissions in China, 1990-2009. *Atmos. Environ.* 60: 1–8.

Li, X.H., Wang, S.X., Duan, L., Hao, J.M., Li, C., Chen, Y.S. and Yang, L. (2007). Particulate and trace gas emissions from open burning of wheat straw and corn stover in China. *Environ. Sci. Technol.* 41: 6052–6058.

Li, Y.Y., Chang, M., Ding, S.S., Wang, S.W., Ni, D. and Hu, H.T. (2017). Monitoring and source apportionment of trace elements in PM$_{2.5}$: Implications for local air quality management. *J. Environ. Manage.* 196: 16–25.

Lin, P., Hu, M., Deng, Z., Slanina, J., Han, S., Kondo, Y., Takegawa, N., Miyazaki, Y., Zhao, Y. and Sugimoto, N. (2009). Seasonal and diurnal variations of organic carbon in PM$_{2.5}$ in Beijing and the estimation of secondary organic carbon. *J. Geophys. Res.* 114: 1013–1033.

Liu, J., Mauzerall, D.L., Chen, Q., Zhang, Q., Song, Y., Peng, W., Klimont, Z., Qiu, X.H., Zhang, S.Q., Hu, M., Lin, W.L., Smith, K.R. and Zhu, T. (2016). Air pollutant emissions from Chinese households: A major and underappreciated ambient pollution source. *PNAS.* 113: 7756–7761.

Liu, P.F., Zhang, C.L., Xue, C.Y., Mu, Y.J., Liu, J.F., Zhang, Y.Y., Tian, D., Ye, C., Zhang, H.X. and Guan, J. (2017). The contribution of residential coal combustion to atmospheric PM$_{2.5}$ in northern China during winter. *Atmos. Chem. Phys.* 17: 11503–11520.

Ma, Z.H., Liang, Y.P., Zhang, J., Zhang, D.W., Shi, A.J., Hu, J.N., Lin, A.G., Feng, Y.J., Hu, Y.Q. and Liu, B.X. (2015). PM$_{2.5}$ profiles of typical sources in Beijing. *Acta Sci. Circumst.* 35: 4043–4052. (in Chinese)

Minguillón, M.C., Perron N., Querol, X., Szidat, S., Fahrni, S.M., Alastuey, A., Jimenez, J.L., Mohr C., Ortega, A.M., Day, D.A., Lanz, V.A., Wacker, L., Reche, C., Cusack, M., Amato, F., Kiss, G., Hoffer, A., Decesari, S., Moretti, F., Hillamo, R., Teinilä, K., Seco, R., Peñuelas, J., Metzger, A., Schallhart, S., Müller, M., Hansel, A., Burkhart, J. F., Baltensperger1, U. and Prévôt, A.S.H. (2011). Fossil versus contemporary sources of fine elemental and organic carbonaceous particulate matter during the DAURE campaign in Northeast Spain. *Atmos. Chem. Phys.* 11: 12067–12084.

Na, K. and Cocker, D.R. (2009). Characterization and source identification of trace elements in PM$_{2.5}$ from Mira Loma, Southern California. *Atmos. Res.* 93: 793–800.

Pachon, J.E., Weber, R.J., Zhang, X., Mulholland, J.A. and Russell, A.G. (2013). Revising the use of potassium (K) in the source apportionment of PM$_{2.5}$. *Atmos. Pollut. Res.* 4: 14–21.

Pant, P., Shukla, A., Kohl, S.D., Chow, J.C., Waston, J.G. and Harrisom, R.M. (2015). Characterization of ambient PM$_{2.5}$ at a pollution hotspot in New Delhi, India and inference of sources. *Atmos. Environ.* 109: 178–189.

Park, S.S., Jung, S.A., Gong, B.J., Cho, S.J. and Lee. S.J. (2013). Characteristics of PM$_{2.5}$ haze episodes revealed by highly time-resolved measurements at an air pollution

monitoring supersite in Korea. *Aerosol Air Qual. Res.* 13: 957–976.

Phillips-Smith, C., Jeong, C.H., Healy, R.M., Dabek-Zlotorzynska, E., Celo, V., Brook, J.R. and Evans, G. (2017). Sources of particulate matter in the Athabasca oil sands region: Investigation through a comparison of trace element measurement methodologies. *Atmos. Chem. Phys.* 17: 9435–9449.

Pio, C.A., Legrand, M., Alves, C.A., Oliveira, T., Afonso, J., Caseiro, A., Puxbaum, H., Sanchez-Ochoa, A. and Gelencsér, A. (2008). Chemical composition of atmospheric aerosols during the 2003 summer intense forest fire period. *Atmos. Environ.* 42: 7530–7543.

Salameh, D., Detournay, A., Pey, J., Pérez, N., Liguori, F., Saraga, D., Bove, M.C., Brotto, P., Cassola, F., Massabò, D., Latella, A., Pillon, S., Formenton, G., Patti, S., Armengaud, A., Piga, D., Jaffrezo, J.L., Bartzis, J., Tolis, E., Prati, P., Querol, X., Wortham, E. and Marchand, N. (2015). $PM_{2.5}$ chemical composition in five European Mediterranean cities: A 1-year study. *Atmos. Res.* 155: 102–117.

Schauer, J.J., Kleeman, M.J., Cass, G.R. and Simoneit, B.R. (2002). Measurement of emissions from air pollution sources. 4. C_1-C_{27} organic compounds from cooking with seed oils. *Environ. Sci. Technol.* 36: 567–575.

Shen, Z.X., Sun, J. Cao, J.J., Zhang, L.M., Zhang, Q., Lei, Y.L., Cao, J.J., Huang, R.J., Liu, S.X., Huang, Y.H., Zhu, C.S., Xu, H.M., Zheng, C.L., Liu, P.P. and Xue, Z.G. (2016). Chemical profiles of urban fugitive dust $PM_{2.5}$ samples in Northern Chinese cities. *Sci. Total Environ.* 569: 619–626.

Song, Y., Zhang, Y.H., Xie, S.D., Zeng, L.M., Zheng, M., Salmon, L.G., Shao, M. and Slanina, S. (2006). Source apportionment of $PM_{2.5}$ in Beijing by positive matrix factorization. *Atmos. Environ.* 40: 1526–1537.

Sun, Y.L., Zhuang, G.S., Wang, W.J., Wang, Y. and Zhang, Y.H. (2006). Characteristics and sources of lead pollution after phasing out leaded gasoline in Beijing. *Atmos. Environ.* 40: 2973–2985.

Tao, J., Gao, J., Zhang, L., Zhang, R., Che, H., Zhang, Z., Jing, J., Cao, J. and Hsu, S.C. (2014). $PM_{2.5}$ pollution in a megacity of southwest China: source apportionment and implication. *Atmos. Chem. Phys.* 14: 8679–8699.

Tao, J. Zhang, L.M., Cao, J.J., Zhong, L.J., Chen, D.S., Yang, Y.H., Chen, D.H., Chen, L.G., Zhang, Z.S., Wu, Y.F., Xia, Y.J., Ye, S.Q. and Zhang, R.J. (2017). Source apportionment of $PM_{2.5}$ at urban and suburban areas of the Pearl River Delta region, south China - With emphasis on ship emissions. *Sci. Total Environ.* 574: 1559–1570.

Tian, H.Z., Wang, Y., Xue, Z.G., Cheng, K., Qu, Y.P., Chai, F.H. and Hao, J.M. (2010). Trend and characteristics of atmospheric emissions of Hg, As, and Se from coal combustion in China, 1980–2007. *Atmos. Chem. Phys.* 10: 11905–11919.

Tian, H.Z., Zhu, C.Y., Cao, J.J., Cheng, K., Hao, J.M., Wang, K., Hua, S.B., Wang, Y. and Zhou, J.R. (2015). Quantitative assessment of atmospheric emissions of toxic heavy metals from anthropogenic sources in China: historical trend, spatial distribution, uncertainties, and

control policies. *Atmos. Chem. Phys.* 15: 10127–10147.

Tian, J. (2016). *Laboratory study on emission characteristics of $PM_{2.5}$ from crop residue burning and residential coal combustion in China*. The university of Chinese Academy of Science, China. (in Chinese)

Wang, S.X., Zhao, X.J., Li, X.H., Wei, W. and Hao, J.M. (2009). Emission characteristics of fine particles from grate firing boilers *Environ. Sci.* 30: 963–968. (in Chinese)

Wang, W., Maenhaut, W., Yang, W., Liu, X.D., Bai, Z.P., Zhang, T., Claeys, M., Cachier, H., Dong, S.P. and Wang, Y. (2014). One-year aerosol characterization study for $PM_{2.5}$ and PM_{10} in Beijing. *Atmos. Pollut. Res.* 5: 554–562.

Wang, Y.X. (2016). *Study on source profiles and risk assessment of heavy metals in power plants coal dust.* Taiyuan University of Technology, China. (in Chinese)

Watson, J.G., Chow, J.C. and Houck, J.E. (2001). $PM_{2.5}$ chemical source profiles for vehicle exhaust, vegetative burning, geological material, and coal burning in Northwestern Colorado during 1995. *Chemosphere.* 43: 1141–1151.

Wu, Z.J., Hu, M., Lin, P., Liu, S., Wehner, B. and Wiedensohler, A. (2008). Particle number size distribution in the urban atmosphere of Beijing, China. *Atmos. Environ.* 42: 7967–7980.

Xu, W.S, Zhang, D.W., Li, Y.T., Chen, T. and Wu, Q.Z. (2016). Variation of $PM_{2.5}$ concentration during two dust pollution events in Beijing. *Clim. Environ. Res.* 21: 78–86. (in Chinese)

Yan, C., Yu, J., Zhao, Y. and Zheng, M. (2017). Biomass burning sources in China, In *Air pollution in eastern Asia: An integrated perspective*, Bouarar, I., Wang, X. and Brasseur, G.P. (Eds.), Springer International Publishing, Cham, pp. 135–166.

Young, L.H., Li, C.H., Lin, M.Y., Hwang, B.F., Hsu, H.T., Chen, Y.C., Jung, C.R., Chen, K.C., Cheng, D.H., Wang, V.S., Chiang, H.C. and Tsai, P.J. (2016). Field performance of a semi-continuous monitor for ambient $PM_{2.5}$ water-soluble inorganic ions and gases at a suburban site. *Atmos. Environ.* 144: 376–388.

Yu, L.D., Wang, G.F., Zhang, R.J., Zhang, L.M., Song, Y., Wu, B.B., Li, X.F., An, K. and Chu, J.H. (2013). Characterization and source apportionment of $PM_{2.5}$ in an urban environment in Beijing. *Aerosol Air Qual. Res.* 13: 574–583.

Zhang, N., Han, B., He, F., Xu, J., Zhao, R.J., Zhang, Y.J. and Bai, Z.P. (2017). Chemical characteristic of $PM_{2.5}$ emission and inhalational carcinogenic risk of domestic Chinese cooking. *Environ. Pollut.* 227: 24–30.

Zhang, R., Jing, J., Tao, J., Hsu, S.C., Wang, G., Cao, J., Lee, C.S.L., Zhu, Z., Chen, Z., Zhao, Y. and Shen, Z. (2013a). Chemical characterization and source apportionment of $PM_{2.5}$ in Beijing: Seasonal perspective. *Atmos. Chem. Phys.* 13: 7053–7074.

Zhang, T., Peng, L., Li, Y.H., Liu, H.L., Wang, Y.X. and Wang, Y. (2016). Chemical characteristics of $PM_{2.5}$ emitted from cooking fumes. *Res. Environ. Sci.* 29: 183–191. (in Chinese)

Zhang, X., Hecobian, A., Zheng, M., Frank, N.H. and Weber, R.J. (2010). Biomass burning impact on PM$_{2.5}$ over the southeastern US during 2007: Integrating chemically speciated FRM filter measurements, MODIS fire counts and PMF analysis. *Atmos. Chem. Phys.* 10: 6839–6853.

Zhang, Y.S., Shao, M., Lin, Y., Luan, S.J., Mao, N., Chen, W.T. and Wang, M. (2013b). Emission inventory of carbonaceous pollutants from biomass burning in the Pearl River Delta region, China. *Atmos. Environ.* 76: 189–199.

Zhang, Z.G., Gao, Q.X., Jiao, M.Y., Bi, B.G., Yan, H. and Ren, Z.H. (2007). Analysis on source locations and transportation paths of sand-dusts affecting Beijing. *Res. Environ. Sci.* 20: 21–27. (in Chinese)

Zhang. R., Cao, J.J., Tang, Y.R., Arimoto, R., Shen, Z.X., Wu, F., Han, Y.M., Wang, G.H., Zhang, J.Q. and Li, G.H. (2014). Elemental profiles and signatures of fugitive dusts from Chinese deserts. *Sci. Total Environ.* 472: 1121–1129.

Zheng, M., Zhang, Y.J., Yan, C.Q., Zhu, X.L., Schauer, J.J. and Zhang, Y.H. (2014). Review of PM$_{2.5}$ source apportionment methods in China. *Acta Sci. Nat. Univ. Pekin.* 50: 1141–1154. (in Chinese)

Zhou, T., Yan, C.Q., Li, X.Y., Cai, J., Guo, X.S., Wang, R., Wu, Y.S., Zeng, L.M., Zhu, T., Zhang, Y.H. and Zheng, M. (2017b). Chemical characteristics and sources of PM$_{2.5}$ in urban and rural sites in the North China Plain during summer. *China Environ. Sci.* 37: 3227–3236. (in Chinese)

Zhou, T., Zhang, B.Y., Yan, C.Q., Li, X.Y., Yu, J.T. and Zheng, M. (2017a). Comparison of water-soluble ions and elements in PM$_{2.5}$ between offline and online measurements in Beijing in winter. *J. Environ. Sci.-China, in Review*.

Zíková, N., Wang, Y.G., Yang, F.M., Li, X.H., Tian, M. and Hopke, P.K. (2016). On the source contribution to Beijing PM$_{2.5}$ concentrations. *Atmos. Environ.* 134: 84–95.